A sequential partly-iterative approach for multicomponent reactive transport with CORE^{2D}

Javier Samper[1], Tianfu Xu[2] and Changbing Yang[1]*

[1] University of La Coruña, La Coruña, Spain, 15071 (corresponding author Javier Samper: jsamper@udc.es)

[2] Lawrence Berkeley National Laboratory, Berkeley, California

* Now at Utah State University. USA. yangcb@gmail.com

Abstract

CORE^{2D} V4 is a finite element code for modeling partly or fully saturated water flow, heat transport and multicomponent reactive solute transport under both local chemical equilibrium and kinetic conditions. It can handle coupled microbial processes and geochemical reactions such as acid-base, aqueous complexation, redox, mineral dissolution/precipitation, gas dissolution/exsolution, ion exchange, sorption via linear and nonlinear isotherms, sorption via surface complexation. Hydraulic parameters may change due to mineral precipitation/dissolution reactions. Coupled transport and chemical equations are solved by using sequential iterative approaches. A sequential partly-iterative approach (SPIA) is presented which improves the accuracy of the traditional sequential noniterative approach (SNIA) and is more efficient than the general sequential iterative approach (SIA). While SNIA leads to a substantial saving of computing time, it introduces numerical errors which are especially large for cation exchange reactions. SPIA improves the efficiency of SIA because the iteration between transport and chemical equations is only performed in nodes with a large mass transfer between solid and liquid phases. The efficiency and accuracy of SPIA are compared to those of SIA and SNIA using synthetic examples and a case study of reactive transport through the Llobregat Delta aquitard in Spain. SPIA is found to be as accurate as SIA while requiring significantly less CPU time. In addition, SPIA is much more accurate than SNIA with only a minor increase in computing time. A further enhancement of the efficiency of SPIA is achieved by improving the efficiency of the Newton-Raphson method used for solving chemical equations. Such an improvement is obtained by working with increments of log-concentrations and ignoring the terms of the Jacobian matrix containing derivatives of activity coefficients. A proof is given for the symmetry and non-singularity of the Jacobian matrix. Numerical analyses performed with synthetic examples confirm that these modifications improve the efficiency and convergence of the iterative algorithm.

Key words: numerical model, reactive transport, sequential iteration, CORE,

1. Introduction

Progress in coupled thermal, hydrodynamic, geochemical and microbial models in porous and fracture media is essential to understand how physical, geochemical and biological reactions are coupled in groundwater and their effect on groundwater-chemistry evolution and the reactive transport of contaminants and microorganisms. Numerical models have been increasingly used for this purpose, a trend that will continue because more sophisticated models and codes are being developed and computer costs keep decreasing. Significant efforts and attempts have been made during recent years toward the development of such tools (Kirkner *et al.*, 1985; Kaluarachchi and Parker, 1990; Steefel and Van Cappellen, 1990; Lensing *et al.*, 1994; Salvage and Yeh, 1998; Ayora *et al.*, 1998; Steefel and Lichtner, 1998; Tebes-Stevens *et al.*, 1998; Yabusaki *et al.*, 1998; Chilakapati *et al.*, 2000; Saaltink *et al.*, 2000; Xu *et al.*, 2000; Yeh, 2000; Ginn *et al.*, 2001; Regnier *et al.*, 2002; Saaltink *et al.*, 2003; Pruess *et al.*, 2004; Maher *et al.*, 2006; Yang, 2006; Yang *et al.*, 2007; Yang *et al.*, 2008a,b). A recent review on reactive transport modelling is presented by Steefel *et al.*(2005).

The group of University of La Coruña (UDC) has developed over the last 15 years a series of codes with the generic name of CORE (COde for modeling partly or fully saturated water flow, heat transport and multicomponent REactive solute transport under both local chemical equilibrium and kinetic conditions). The reference code, CORE-LE^{2D} was an extended and improved version of a previous reactive transport code, TRANQUI (Xu *et al.*, 1999). CORE-LE^{2D} solves simultaneously for groundwater flow, heat transport and multicomponent reactive solute transport under the following conditions: 1) 2-D confined or unconfined, saturated or unsaturated steady-state or transient groundwater flow with general boundary conditions. 2) Chemical equilibrium including (a) Acid-base, (b) Redox, (c) Aqueous complexation, (d) Surface sorption, (e) Ion exchange, (f) Mineral dissolution-precipitation, and (g) Gas dissolution-

exsolution. 3) Transient heat transport considering conduction, heat dispersion and convection. CORE^{2D}V2 was released in 2000 (Samper *et al.*, 2000). Contrary to CORE-LE^{2D}, CORE^{2D}V2 can handle kinetically-controlled dissolution-precipitation reactions. This version has been widely verified (Samper *et al.*, 2000). CORE^{2D} V2 was the base for the development of: 1) INVERSE-CORE^{2D}, a code for automatic estimation of up to 16 different types of reactive transport parameters (Dai and Samper, 2004, 2006) and 2) BIOCORE^{2D} (Zhang, 2001; Samper *et al.*, 2006a; Zhang *et al.*, 2008), a code which accounts for microbial processes in addition to geochemical reactions.

The most recent version of CORE^{2D}, CORE^{2D} V4 (Samper *et al.*, 2003) is presented here. It was developed from CORE^{2D} V2 (Samper *et al.*, 2000) by adding some of the capabilities of BIOCORE^{2D} and INVERSE-CORE^{2D} such as automatic time stepping, kinetic aqueous complexation reactions, microbial processes, and inverse subroutines of INVERSE-CORE^{2D}. A novel sequential approach is presented here which requires iteration between transport and chemical equations only in finite element nodes having a large mass transfer between solid and liquid phases. This approach is denoted as sequential partly-iterative approach (SPIA). At a given time step, after solving the transport equations, chemical calculations are performed only at the nodes not satisfying a prescribed partly-iterative tolerance. The computing time and the accuracy of SPIA is compared to those of other sequential iterative approaches for several 1-D synthetic examples covering the major types of hydrochemical reactions and a case study reported by Xu *et al.* (1999) dealing with cation chromatographic separation through the Llobregat Delta aquitard near Barcelona, Spain. Several modifications of standard Newton-Raphson iterative methods used for solving the set of nonlinear chemical equations are proposed which include: (1) working with increments of log-concentrations and (2) ignoring the terms of the Jacobian matrix containing derivatives of activity coefficients with respect to component concentrations. These modifications are shown to improve the efficiency and convergence of the

iterative algorithm and lead to better conditioned systems of equations. A proof is given for the symmetry and nonsingularity of the Jacobian. Numerical analyses performed with synthetic examples confirm these results.

2. Mathematical formulation

When diffusion and dispersion coefficients are the same for all aqueous species, reactive transport equations can be written in terms of total dissolved component concentrations, C_k, as (Yeh, 2000):

$$\nabla \cdot (\theta \mathbf{D} \nabla C_k) - \mathbf{q} \cdot \nabla C_k + w(C_k^* - C_k) + \theta R_k = \theta \frac{\partial C_k}{\partial t} \quad k = 1, 2, ..., N_C \qquad (1)$$

where **D** is the dispersion tensor, **q** is the Darcy velocity, θ is the volumetric water content, w is the external fluid source term, C^* is the dissolved concentration of external fluid sources, k refers to the chemical component from 1 to N_C. R_k is the reactive chemical-microbial sink/source term which includes the chemical interactions of the k^{th} component with the solid and gaseous species, the kinetics of aqueous complexation reactions and the consumption/production of the chemical component by microbiological processes.

Geochemical reactions can be grouped into two classes: 1) Homogeneous reactions which occur in the liquid phase, such as aqueous complexation, acid-base and redox reactions and 2) Heterogeneous reactions which involve mass transfer from liquid to solid/gas phases, and include mineral precipitation/dissolution, surface complexation, cation exchange and gas dissolution/exsolution. The total dissolved concentration of a given component, C_k in Eq. (1) can be written in an explicit form as a function of the concentration of the N_C components or primary species

$$C_k = c_k + \sum_{j=1}^{N_x} \nu_{jk} x_j = c_k + \sum_{j=1}^{N_x} \nu_{jk} K_j^{-1} \gamma_j^{-1} \prod_{i=1}^{N_c} c_{ji}^{\nu_{ji}} \gamma_i^{\nu_{ji}} \qquad (2)$$

where K_j is the equilibrium constant which depends on the pressure and temperature of the system; x_j and c_i are molar concentrations of secondary and primary species, respectively, γ are activity coefficients, N_x is the number of secondary species, and ν_{ij} is stoichiometric coefficient of the *i*-th primary species in aqueous complexation of the *j*-th secondary species.

Under equilibrium conditions, dissolution-precipitation reactions can be described by the mass action law which states that

$$X_m \lambda_m K_m = \prod_{i=1}^{N_c} c_i^{\nu_{mi}^p} \gamma_i^{\nu_{mi}^p} \tag{3}$$

where X_m is molar fraction of the *m*-th solid phase; λ_m is thermodynamic activity coefficient (X_m and λ_m are taken equal to unity for pure phases); ν_{mi}^p is the stoichiometric coefficient in the dissolution reaction of the *m*-th solid phase; and K_m is the corresponding equilibrium constant. The assumption of pure phases has been accepted for reactive transport problems involving cement-based materials (Richardson, 1999). The equilibrium condition provides a relationship between the concentrations of the involved aqueous species. The mass transfer needed to achieve this condition is not specified. In fact, Eq. (3) does not include the concentration of the *m*-th solid phase, and therefore the amount of dissolved/precipitated mineral cannot be computed explicitly.

Kinetic mineral dissolution/precipitation is modeled with the following rate law:

$$r = \varsigma e^{-\frac{Ea}{RT}} \sum_{k=1}^{N_k} K_k \prod_{i=1}^{N_C+N_X} a^{ki} (\Omega^{\theta_k} - 1)^{\eta_k} \tag{4}$$

where r is the dissolution/precipitation rate (mol/m^2/ s), Ω is the saturation index (dimensionless) and ς is an integer variable which takes values of 1 or –1 depending on whether Ω is larger or smaller than 1 (precipitation/dissolution), respectively. At equilibrium $\Omega = 1$ and $r = 0$. The term $e^{-\frac{Ea}{RT}}$ is a thermodynamic factor which accounts for the temperature, T, and the apparent activation energy of the overall reaction Ea (KJ/mol). R (KJ/mol·°K) is the gas constant and T is

the absolute temperature. N_k is the number of kinetic reaction terms. K_k is the kinetic rate constant for the kth kinetic term (mol/m^2/s), $\prod_{i=1}^{N_C+N_X} a^{ki}$ is a term accounting for the catalytic effect of some species such as H^+ and a_i is the activity of the ith aqueous species. N_C and N_X are the numbers of primary and secondary species, respectively, θ_k and η_k are kinetic parameters usually determined from experiments.

The subsurface environment contains microbes which use organic and inorganic chemical species as substrates, electron acceptors and nutrients. Microbial growth obeys Monod kinetic laws such as

$$\frac{\partial C_b^i}{\partial t}\Big|_{growth} = \sum_{p=1}^{N_s}\sum_{q=1}^{N_a}\sum_{r=1}^{N_n} \mu_i^{p,q,r} C_b^i G_i^{p,q,r} \frac{C_s^p}{K_s^p + C_s^p}\frac{C_a^q}{K_a^q + C_a^q}\frac{C_n^r}{K_n^r + C_n^r} \qquad (5)$$

where C_s, C_a and C_n are concentrations of substrates, electron acceptors, nutrients, respectively; K_s, K_a, K_n are half-saturation constants of substrates, electron acceptors and nutrients, respectively; superscripts p, q and r refer to the order of substrates, electron acceptors and nutrients in the ecosystem; $\mu_i^{p,q,r}$ is the specific growth rate and $G_i^{p,q,r}$ is the lag coefficient of the i^{th} microbe growing on the p^{th} substrate and q^{th} electron acceptor; and N_s, N_a, and N_n are the total numbers of substrates, electron acceptors and nutrients, respectively. Expressions of other microbial processes such as metabolic competition, decay, metabiosis, endogeneous respiration and attachment/detachment of microorganisms on biofilm can be found in Zhang (2001) and Samper *et al.* (2006a). Consumption and yield rates of chemical species involved in microbiological processes are related to microbial growth rates by yield coefficients. The rate of consumption of the *p*th substrate due to microbial growth, B_p, is given by:

$$B_p = \frac{\partial C_s^p}{\partial t} = -\sum_{i=1}^{N_b}\sum_{j=1}^{N_b^i} \frac{1}{Y_s^{i,j,p}} \frac{\partial C_b^i}{\partial t}\Big|_{growth} \qquad (6)$$

where $Y_s^{i,j,p}$ is the yield coefficient of the *p*th substrate being used by the *i*th microbe in its *j*th growth. To illustrate the previous concepts, let us consider iron reducing bacteria (IRB) which grow at a rate R_B by oxidizing dissolved organic carbon (DOC) and reducing ferric minerals. The rate of substrate consumption, R_{DOC}, is given by

$$R_{DOC} = -\frac{R_B}{Y_B} \qquad (7)$$

where Y_B is the yield coefficient of DOC to IRB. Oxidation of DOC yields bicarbonate. Then, the rate of bicarbonate production by microbial processes, $R_{HCO_3^-}$, is calculated as $R_{HCO_3^-} = -Y_{HCO_3^-} R_{DOC}$ where $Y_{HCO_3^-}$ is the yield coefficient of HCO_3^- from DOC. The consumption rate of dissolved Fe^{3+}, $R_{Fe^{3+}}$, is given by $R_{Fe^{3+}} = f_a R_{DOC}$ where f_a is the proportionality coefficient of Fe^{3+} and DOC in the redox reaction. Proportionality coefficients are generally equal to stoichiometric coefficients. However, they may differ from stoichiometric coefficients when the substrate is a complex macromolecular organic compound.

Chemical reactions which involve mass transfer from solid to liquid phases can induce changes in physical and hydrodynamic properties of a porous medium (Steefel and Lichtner, 1994). For instance, mineral dissolution (precipitation) can increase (decrease) the porosity. Such a change in porosity may, in turn, affect flow and transport properties (e.g., diffusion coefficient and permeability). Changes in porosity are evaluated from computed dissolution/precipitation rates using an explicit method. CORE^{2D} V4 incorporates a Kozeny-Carman equation to relate permeability to porosity. Effective diffusion coefficient may change with porosity of the porous medium due to mineral dissolution-precipitation. Different expressions of effective diffusion coefficient in terms of porosity have been implemented in CORE^{2D} V4. One of them is the expression derived by Garboczi and Bentz (1992) from numerical tests performed of microstructure of cement paste.

3. Numerical methods

The finite element method is used in CORE^{2D} V4 to solve for groundwater flow, solute and heat transport equations. The groundwater flow equation is solved first in terms of hydraulic heads for saturated flow in confined or unconfined aquifers. Unconfined aquifer flow equation is solved iteratively using a predictor-corrector scheme. Flow in variably saturated media is solved in terms of pressure heads by a Newton-Raphson iterative method. For steady-state flow, the equation is solved once only at the first time step. Water velocities, which are needed to evaluate advective and dispersive solute and heat fluxes, are computed from nodal head values by direct application of Darcy's law to the finite element solution.

Thermal conduction and advection are considered in the heat equation. The solution of the heat transport equation is used to update temperature-dependent chemical equilibrium constants, activity coefficients and kinetic rates. Solution of heat transport shares subroutines with solute transport solution because the structure of both equations is similar.

Each chemical component has a transport equation in terms of its total dissolved concentration. Since chemical sink/source terms are assumed known (they are evaluated at the previous iteration), each transport equation can be solved separately. Transport matrices may be different for each component because diffusion coefficients and effective porosity may be component dependent. A Newton-Raphson method is used to solve the geochemical equations. Biogeochemical reactions are solved node-wise.

The numerical formulation presented here to solve the coupled equations of solute transport and chemical reactions is based on the sequential iteration approach (SIA) (Yeh and Tripathi, 1991; Simunek and Suarez, 1994; Walter *et al.*, 1994; Lichtner, 1996; Xu *et al.*, 1999) in which transport and chemical equations are solved separately in a sequential manner. Transport equations are solved first and then chemical reactions. This sequence is repeated until

convergence is attained for a prescribed tolerance. The key point of SIA is therefore the sequential solution of two independent sets of equations: (a) transport equations which are solved in a component manner, and (b) chemical equations which are solved node wise. These two sets of equations are coupled by reaction sink/source terms which are updated during the iterative cycle. The formulation implemented in CORE uses a mixed explicit-implicit scheme based on the standard transport operator which has adequate convergence properties (Xu, 1996). This scheme derives from rewriting Eq. 1 as

$$\nabla \cdot \left(\theta \mathbf{D} \nabla C_j^{s+1/2} \right) - \mathbf{q} \cdot \nabla C_j^{s+1/2} + w\left(C_j^{*} - C_j^{s+1/2} \right) + \theta R_j^{s} = \theta \frac{\partial C_j^{s+1/2}}{\partial t} \qquad j = 1, \ldots, N_C \quad (8)$$

where superscript *s* denotes the transport plus reaction iteration number. A transport plus reaction iteration consists of two stages, a transport stage denoted by *s*+½ (it should be noticed that ½ does not mean Δt/2 where Δt is the time step) and a reaction stage denoted by *s* +1. Since reaction sink/source terms R_j^s do not depend on $\mathbf{C}_j^{s+1/2}$, Eq. 8 are linear and have the same structure as the standard transport equation of a conservative solute. These equations are solved with the Galerkin finite element method (Xu, 1996) and using a finite difference backwards Euler scheme for time derivatives. The system of equations for the j-th component is

$$\left[\eta \mathbf{E} + \frac{\mathbf{F}}{\Delta t} \right] \mathbf{C}_j^{k+1,s+1/2} = \mathbf{g}_j^{k+1} + \mathbf{R}_j^{k+1,s} + \left[(\eta - 1)\mathbf{E} + \frac{\mathbf{F}}{\Delta t} \right] \mathbf{C}_j^{k} \quad (9)$$

where η is a time weighting parameter (η=0 for explicit, η=1 for implicit), **E** is a (N_d x N_d) matrix containing dispersion and advection terms where N_d is the number of nodes of the finite element grid, **F** is also a (N_d x N_d) matrix of storage terms, $\mathbf{C}_j^{k+1,s+1/2}$ is a column vector of nodal concentrations at the (s+1/2) stage of the (k+1)-th time step, $\mathbf{R}_j^{k+1,s}$ is the column vector of reaction sink/source terms which are derived from the solution of the chemical system at the s-th iteration, $\mathbf{g}_j^{k+1}$ is a column vector containing boundary terms as well as external fluid sink/source

terms, $\Delta t = t^{k+1} - t^{k}$, and superscript k denotes time step. The actual expressions of **E, F** and $\mathbf{g}_j^{k+1}$ are given by *Xu* (1996). Eq. 9 is solved separately for each chemical component. Computed component concentrations, $\mathbf{C}_j^{k+1,s+1/2}$, are then used to update total analytical concentrations, $\mathbf{T}_j^{k+1,s+1/2}$, which are defined in (A1) and include the contributions of precipitated, exchanged and sorbed species in addition to total dissolved concentrations. By solving the chemical equations in the manner described in Appendix A one obtains new values of dissolved concentrations $\mathbf{C}_j^{k+1,s+1}$ and reaction terms $\mathbf{R}_j^{k+1,s+1}$ which are compared to $\mathbf{C}_j^{k+1,s+1}$ and $\mathbf{R}_j^{k+1,s}$ to check for convergence. Sequential solution of transport and chemical equations is repeated until prescribed convergence criteria are satisfied both in terms of dissolved concentrations and reactive terms.

The sequential non-iterative approach (SNIA) is a particular case of the sequential iteration approach (SIA) in which the sequence of transport and reaction equations is solved only once. The sequential partly-iterative approach (SPIA) only requires iteration between transport and chemical equations in areas where there is a large mass transfer between the solid and the liquid phases.

The time step Δt can be specified in advance by the user or derived from an automatic time stepping algorithm. The initial value of Δt is obtained as the minimum value which satisfies simultaneously the following conditions: 1) The dimensionless time needed for the dissipation of a hydraulic perturbation within any finite element should be smaller than 2, 2) Courant number smaller than one, 3) Stability of chemical kinetics and 4) User-specified minimum printing intervals. Time steps are automatically updated by using empirically-derived expressions derived from several functions measuring the convergence performance such as numerical stability, number of transport+chemistry iterations and maximum cumulative concentration change among all nodes and aqueous components. Further details of the stepping algorithm can be found in Zhang (2001).

Two types of stabilization methods have been implemented in CORE^{2D} V4 to reduce numerical oscillations produced by classical finite element methods when solving advection-dominated problems, They include stream upwinding Petrov-Galerkin (SUPG) method and subgrid scale stabilized method (Yang and Samper, 2008).

CORE^{2D} V4 can cope with heterogeneous systems having irregular internal and external boundaries. The code also can handle heterogeneous and anisotropic media. It is not restricted to specific chemical species, and therefore can consider any number of aqueous, exchanged and sorbed species, minerals and gases. Thermodynamic data and stoichiometric coefficients of chemical equilibrium reactions are read directly from a database which is modified from the EQ3NR database (Wolery, 1992). A pre-processor is provided to convert the contents of other chemical databases such as PHREEQE, MINTEQ, NEA, CHEMVAL and HATCHES into the format of CORE databases. It is worthy noting that CORE^{2D} V4 can handle also problems with: 1) Anisotropic diffusion to deal with diffusion anisotropy in clay media (see Samper *et al.*, 2006b), 2) Isotopic transport coupled with chemical reactions for the purpose of simulating radionuclide release from a radioactive waste repository, and 3) Automatic estimation of flow, solute transport, chemical and biological parameters (Yang *et al.*, 2008b).

4. Verification and Applications of CORE

CORE^{2D} V4 has been extensively verified against analytical solutions. The conservative solute and heat transport subroutines of CORE^{2D} V4 have been verified for one-dimensional conditions. The 1-D test case corresponds to the time evolution of concentrations in a semi-infinite confined aquifer under steady-state uniform flow. Reactive transport with kinetic dissolution-precipitation reactions and kinetic aqueous complexation has been verified against analytical solutions for 1-D problems in saturated media (Yang and Samper, 2008).

Multicomponent reactive transport coupled with cation exchange reactions has been verified against analytical solutions derived by Samper and Yang (2007). Reactive transport with kinetic rate laws was verified for calcite and smectite dissolution against 1DREACT (Steefel, 1993). Capabilities of CORE^{2D} V4 to deal with redox reactions were verified against DYNAMIX with a case of uranium migration through a column (Liu and Narasimhan, 1989). Reactive transport with cation exchange routines was verified against a solution reported in PHREEQM user's manual problem (Nienhuis *et al.*, 1991) which involves a column initially filled with 1 mM $NaNO_3$ and 0.2 mM KNO_3 which is flushed by a 0.6 mM $CaCl_2$ solution. This case illustrates the chromatographic separation of Ca^{2+} and K^+. Ca^{2+} is weakly adsorbed and is eluted first. K^+ is more tenaciously held than Ca^{2+} and appears retarded in the column effluent. As indicated by Samper *et al.*, (2006), subroutines for solving microbial processes were verified against analytical solutions derived by Salvage and Yeh (1998) and against other codes such as BIOCLOG3D (Engesgaard, 2000) and FEREACT (Tebes-Stevens *et al.*, 1998).

CORE^{2D} V4 has been extensively used to model laboratory experiments (Samper *et al.*, 2008a,b) and *in situ* experiments performed at Underground Rock Laboratories (URL) such as those of Mont Terri (Switzerland) within the context of DI-B (Samper *et al.*, 2006b), DR and VE experiments, Mol (Belgium) in the framework of CERBERUS experiment (Samper *et al.*, 2006a; Zhang *et al.*, 2008), Bure (France) within DIR experiments, Äspö (Sweden) within the Redox Zone (Molinero *et al.*, 2004; Molinero and Samper, 2006) and REX experiments (Yang *et al.*, 2008b) and FEBEX experiment (Samper *et al.*, 2008c) at Grimsel (Switzerland). CORE^{2D} V4 has been used also to calculate the long-term geochemical evolution of radioactive waste repositories in clay (Yang *et al.*, 2008a) and granite (Yang *et al.*, 2007) in integrated performance assessment projects such as BENIPA, NFPRO and PAMINA. CORE^{2D} has been used also to simulate: 1) Solute transport in natural aquifers including uranium transport in Andújar aquifer (Spain), geochemistry of Aquia aquifer, USA (Dai *et al.*, 2006) and salt water

flushing in Llobregat delta aquitard (Dai and Samper, 2006), 2) Drainage of civil engineering works, flow into tunnels and underground excavations, 3) Groundwater flow and heat transport in hydrothermal systems, 4) Concrete degradation (Galíndez *et al.*, 2006), and 5) Stochastic transport and multicomponent competitive cation exchange in aquifers (Samper and Yang, 2006)

5. Comparison of sequential approaches

Some investigators such as Walter *et al.* (1994) claim that physical transport and chemical reaction reactions taking place under equilibrium conditions can effectively be de-coupled and therefore can be solved separately in a sequential manner without the need to iterate between transport and chemical equations. Steefel and MacQuarrie (1996) present a comparison of several approaches including direct substitution approach (DSA), SIA, SNIA and a time-centered SNIA or Strang splitting approach using several simple cases. They found that SIA sometimes gives the smallest error to CPU time ratio although in other cases SNIA is more efficient. While DSA can solve all the problems, it is not always the most computationally efficient approach. Xu *et al.* (1999) present a systematic comparison of the performance and accuracy of SIA and SNIA. Their results show that SNIA requires less computing time than SIA. However, the accuracy of SNIA is highly dependent on space and time discretization and the type of chemical reactions.

A new sequential approach is presented here that requires iteration between transport and chemical equations only in nodes where there is a large mass transfer between the solid and the liquid phases. It is the sequential partly-iterative approach (SPIA). This new approach is implemented as follows. After the transport stage of a given iteration, chemical equations are solved only at the nodes in which the following convergence criterion has not been met in previous iterations

$$\max_{\text{all } j}\left|\frac{\Delta Q_{ij}}{C_{ij}}\right| \le \varepsilon \qquad (10)$$

where C_{ij} is the total dissolved concentration of the j-th chemical component at the i-th node, ΔQ is the mass transfer from the solid to the liquid phase per unit fluid volume during the time step Δt, and ε is a prescribed partly-iterative tolerance. Notice that ΔQ and C_{ij} have the same units because it is a common practice in reactive transport modeling to express all concentrations as mol/L, even for solid species.

To evaluate the performance of SPIA, a systematic comparison of the accuracy and computing requirements of the three sequential approaches (fully iterative, SIA, partly-iterative, SPIA, and non-iterative, SNIA) was carried out. Accuracy of SNIA and SPIA is evaluated by computing relative differences such as,

$$\delta^*_{ijk} = \frac{\left| C^*_{ijk} - C^{SIA}_{ijk} \right|}{\frac{(C^*_{ijk} + C^{SIA}_{ijk})}{2}} \tag{11}$$

where superscript * applies to either SPIA or SNIA, δ^*_{ikj} is the relative difference at the i-th node for the j-th component at the k-th time step. To perform a systematic comparison, only the maximum and average values of δ^*_{ikj}, δ^*_{max} and $\overline{\delta}^*$ are retained which are defined as

$$\delta^*_{max} = \max_{\text{all i, j, and k}} \left(\delta^*_{ijk} \right) \tag{12}$$

$$\overline{\delta^*} = \frac{\sum_{i=1}^{N_d} \sum_{j=1}^{N_C} \sum_{k=1}^{N_t} \delta^*_{ijk}}{N_d \, N_C \, N_t} \tag{13}$$

where N_d, N_C, and N_t are the number of nodes, chemical components and time steps, respectively.

5.1 Comparison using synthetic examples

The comparison of the performance of SIA, SPIA and SNIA was conducted on the same synthetic cases used for TRANQUI verification (Xu, 1996). They correspond to simple 1-D

reactive transport problems under steady-state flow conditions. Each case involves a different type of chemical reactions. The first one deals with gypsum dissolution while the second involves pyrite oxidation. The third case is a cation exchange verification example discussed by Appelo (1994). The forth synthetic case coincides with Case 2 of Cederberg *et al.* (1985) which involves cadmium sorption in a soil column.

Stability of the numerical solutions of solute transport equation as well as convergence of the iterative process are controlled by the Courant and Peclet dimensionless numbers. The Courant number, C, is defined as $v\Delta t / \Delta x$ where v is water velocity and Δt is time increment. In order to ensure stability, C must be less than 1, although usually $C < 1/3$. The Peclet number, P, is the ratio between advective and dispersive transport. If diffusion is negligible, the grid Peclet number is equal to $\Delta x / \alpha$ where Δx is grid size and α is dispersivity. Stability is usually ensured whenever $P < 2$.

A Courant number of 0.1 and a Peclet number of 1 were used in all four cases. The values of the maximum and average differences for each case are summarized in Table 1. For SNIA the maximum and average differences are small (less than 1.16% and 0.4%, respectively) for all cases (dissolution, redox and adsorption) except for cation exchange. Here the average difference is moderately large (equal to 2.4 %) while the maximum difference reaches a significantly large value of 57.4 %. The partly-iterative approach is always much more accurate than SNIA. One can see in Table 1 that SPIA differences are almost negligible. The largest maximum relative difference is equal to 8.4×10^{-4} % (five orders of magnitude smaller than that of SNIA).

The performance of the three approaches in terms of computing time is summarized in Table 2. SIA requires from 1.4 to 3.8 times the CPU time of SNIA which is always the fastest approach. SPIA, which is much more accurate than SNIA, requires from 1.2 to 1.9 times the CPU time of SNIA.

Clearly, SPIA leads to a substantial saving of computing time when compared to the most CPU-demanding approach, while it provides solutions which for all practical purposes are as accurate as those of SIA.

Additional runs were performed for the cation exchange synthetic case because it shows the largest errors. A more detailed account of this example is provided to understand better the results. This case corresponds to a laboratory column experiment reported by Appelo (1994). It illustrates cation chromatographic separation along a column which is initially filled with a pore water containing 1 mM of $NaNO_3$ and 0.2 mM of KNO_3. The column is flushed at a constant discharge of 0.072 m/day with a 0.6 mM $CaCl_2$ solution. The column is 0.1 m long and contains a porous material with a porosity of 0.3, a dispersivity of 0.001 m, and a cation exchange capacity (CEC) of 0.01779 meq/100 g. The density of the solids is equal to 2650 kg/m^3. Molecular diffusion is negligible. Redox reactions which could affect nitrate concentrations are disregarded. Therefore, both nitrate and chloride can be treated as conservative species. Thermodynamic data were taken from PHREEQM database (Nienhuis, 1991).

To evaluate the effect of Courant and Peclet numbers on average and maximum relative differences of SPIA and SNIA, this problem was solved for 12 pairs of Courant and Peclet numbers corresponding to Peclet numbers of 0.2 and 1 and the following Courant numbers: 0.05, 0.1, 0.2, 0.5, 1 and 2.

For the non-iterative approach, SNIA, maximum differences, δ^*_{max}, are much greater than average differences, $\overline{\delta}^*$ (Figure 1). Both of them increase with increasing Courant and Peclet numbers. Differences are much more sensitive to variations in Courant number than they are with respect to P. A log-log plot of average and maximum relative differences versus Courant number reveals that results fit to straight lines having slopes equal to 0.61 for $\overline{\delta}^*$ and 0.44 for δ^*_{max} which are similar for P=0.2 and P=1. The average difference is small (1.5 %) for C = 0.05.

However, it attains a significantly large value (17.2 %) for C = 2. Maximum differences are much greater and vary from 30 % for C = 0.05 to 184 % for C = 2.

A convergence tolerance ε (in Eq. 10) of 10^{-2} was used for the partly-iterative approach, SPIA. Contrary to SNIA, SPIA maximum differences show a mild dependence on the values of C and P. The maximum difference is always smaller than 1.2 %, while the average difference is so small (on the order of 2×10^{-4} %) that it does not show in Figure 1. For $\varepsilon = 10^{-3}$, differences are almost zero, meaning that SPIA and SIA solutions are almost identical.

Figure 2 shows the breakthrough curves computed with the three approaches using Courant and Peclet numbers equal to 1. As expected, all solutions coincide entirely for conservative solutes such as Cl^-. The breakthrough curve of Na^+ is retarded with respect to that of Cl^-. Moreover, K^+ is tied to the exchange complex more strongly than Na^+, and it is released later to the solution. In spite of the fact that the input solution has a very low K^+ concentration, the release of exchanged K^+ provokes a peak of dissolved K^+ (retardation). Dissolved Ca^{2+} coming from the input solution is consumed in displacing Na^+ and K^+ from exchange sites. Therefore, dissolved Ca^{2+} breaks through much later than what would correspond to a conservative species. SPIA results obtained with $\varepsilon = 10^{-2}$ and $\varepsilon = 10^{-3}$ cannot be distinguished from those of SIA in Fig. 2. There are some differences between SNIA and SIA breakthrough curves of K^+. Curves of Na^+ and K^+ computed with SNIA are smoother than those of SIA, indicating that SNIA introduces numerical dispersion. This result is consistent with the findings of Herzer and Kinzelbach (1989) and Valocchi and Malmstead (1992) who concluded from both theoretical and numerical analyses that de-coupling of transport and chemical equations introduces numerical dispersion unless these equations are solved iteratively.

5.2. Comparison on a case study

A case study dealing with cation chromatographic separation through a vertical column of the Llobregat River Delta aquitard (Barcelona, Spain) was used to evaluate the performance of the sequential approaches in real complex problems. The regional setting of this two-layer aquifer separated by the aquitard here considered is described elsewhere (Iribar *et al.*, 1997). The cation content of interstitial water in the Llobregat Delta aquitard shows the typical distribution of saline water in equilibrium with the soil, which is being displaced by upwards fresh water flow. Xu *et al.* (1999) presented the results of the simulation of reactive transport using TRANQUI.

It is believed that the Llobregat River Delta aquifer system has been in close to steady-state head conditions during the last 3500 years. Fresh water coming from the deep aquifer has been flushing the aquitard at an estimated average flux of 2.373×10^{-3} m/year. The 35 m thick saturated aquitard column is constituted by a homogeneous clay-silt layer. According to Manzano (1993), porosity is equal to 0.411, longitudinal dispersivity amounts to 0.7 m while the pore water diffusion coefficient takes a value of 3.2×10^{-3} m^2/year.

The chemical composition of native aquitard pore water is listed in Table 3. This composition coincides for the most part with that of present Mediterranean seawater. Table 3 also contains the chemical composition of groundwater in the lower aquifer. The numerical model accounts for: (1) acid-base and aqueous complexation reactions involving 14 secondary species, (2) cation exchange, and (3) dissolution-precipitation of calcite. These reactions are assumed to take place at local equilibrium. Their corresponding equilibrium constants are listed in Table 4. Gaines-Thomas convention was adopted for cation exchange, according to which activities of exchanged cation are given by their equivalent fractions (Appelo and Postma, 1993). Selectivity coefficients were derived from averages of measured values, except for NH_4^+, for which a value of 0.5 was selected.

Since the performance of SNIA and SPIA compared to that of SIA is expected to depend on space and time discretization, reactive transport through the Llobregat Delta aquitard was solved for a wide range of Peclet, P, and Courant, C, numbers. P ranges from 0.5 to 2 while C varies from 0.0579 to 0.9264.

SNIA introduces errors which increase with increasing values of P and C. In a log-log plot of maximun and average errors versus Courant number, numerical results fit to straightlines (see Figure 3) having of 0.63 for maximum differences and 0.4 for average differences which are similar to those found for the cation exchange case (compare Figures 1 and 3). The Peclet number also affects the magnitude of the differences, although its effect is much smaller than that of the Courant number. For the smallest P and C values (P=0.5 and C= 0.0579) the average difference is rather small (1.32%) while the maximum difference is equal to 16.32 %. For the largest P and C values (P= 2 and C= 0.9264), the average difference takes a small but significant value of 5 % whereas the maximum difference amounts to 123 %.

Numerical results obtained with the partly-iterative approach, SPIA, are for all practical purposes undistinguishable from those of the exact solution. SPIA errors are always close zero, and for that reason they are not plotted in Figure 3.

Common to all approaches is the increase of CPU time when the Courant number decreases (Table 5). Such an increase is especially noticeable for C=0.0579. On the contrary, CPU time shows no clear dependence on Peclet number. One would expect to observe a CPU time reduction by using coarse grids with large Peclet numbers. Some of the results in Table 5 confirm this expectation, although the results corresponding to C=0.0579 show just the contrary. SNIA requires from 2 to 3 times less CPU time than SIA. This means that CPU time is reduced by a factor of 2 to 3 when iteration between transport and chemistry calculations is not performed. It should be noticed that the ratio of SIA to SNIA CPU times decreases as C

decreases. For commonly used values of Courant number (usually less than 1/3), this ratio is approximately equal to 2.

As expected, the CPU time for SPIA is always between those of SNIA and SIA for fixed values of P and C. A comparison of SPIA with the most accurate and time consuming approach, SIA, reveals that SPIA requires from 30 to 50% less CPU time than SIA. The smaller the Courant number, the greater the saving of CPU time achieved by SPIA. Apparently, the reduction in computing time achieved by SPIA seems to be independent of Peclet number, at least within the range $0.5 \leq P \leq 2$. The comparison of the performance of SPIA with respect to that of SNIA shows that SPIA is as efficient as SNIA for small Courant numbers. For values greater than 0.2, however, SPIA requires twice as much CPU time as SNIA.

Figure 4 shows the breakthrough curves of total dissolved Ca^{2+}, K^{+}, Na^{+} and Cl^{-} at several points in the aquitard. They were computed with SNIA, SPIA, and SIA using Courant and Peclet numbers both equal to 1. Similar to the exchange synthetic case, SPIA curves coincide entirely with those of SIA. Numerical solutions obtained with the non-iterative approach, SNIA, also coincide with those of SIA for conservative species such as chloride (see Figure 4d). However, SNIA solutions for strongly reactive species such as calcium, which interacts with the exchange complex and participates in calcite dissolution-precipitation, show some deviations from “exact” solutions. Deviations in Ca breakthrough curves are largest at the bottom of the aquitard where the effects of mixing of fresh and saline waters and chemical reactions are strongest (Figure 4a). Potassium breakthrough curves computed with SNIA also show noticeable discrepancies with respect to SIA. In addition, these curves exhibit additional numerical dispersion. It should be noticed that SNIA solution for sodium (see Figure 4d) shows no major discrepancies because the changes in its concentration are caused mostly by dilution and to a much less extent by cation exchange. To realize such effect, the reader should pay attention to the fact that the concentration scale in Figure 4d is ten times larger than those used in Figures 4a, 4b and 4c.

In general, the largest errors of SNIA take place in areas where boundary water mixes with native water, near concentration moving fronts and at the interfaces between different geochemical zones. To overcome this drawback of SNIA, SPIA iterates between transport and chemical reactions only in regions where it is needed to achieve accurate numerical solutions.

Numerical modelling of reactive transport in the Llobregat Delta aquitard allows us to draw the following conclusions about SIA, SPIA, and SNIA:

1) SNIA is from 2 to 3 times numerically more efficient than SIA. However, SNIA solutions are less accurate and exhibit more numerical dispersion than SIA solutions. SNIA errors increase with increasing Peclet and Courant numbers. Relative errors range from 1.3 to 5% (in average), although they may reach locally very large values.

2) The proposed sequential partly-iterative approach, SPIA, achieves almost the same accuracy as SIA with a reduction in CPU time ranging from 30 to 50%.

3) The accuracy of SPIA solutions depends on the partly-iterative tolerance, ε. Although the optimun value of ε may be problem-dependent, for the Llobregat Delta aquitard a value of $\varepsilon = 10^{-3}$ leads to results which are identical to those of SIA.

6. Numerical aspects of chemical calculations

Most of the CPU time needed to solve the examples presented here is consumed by solving the chemical equations. This holds true for all approaches, including the non-iterative approach. This remark, which agrees with the statements of Yeh and Tripathi (1989), shows that the most effective way to improve the overall numerical efficiency of reactive transport should focus on deriving highly efficient numerical algorithms for the solution of chemical equations. Under local equilibrium conditions, these highly nonlinear equations are solved using the Newton-Raphson iterative method described in Appendix A. The general solution scheme described in Appendix A is used to solve for mineral dissolution/precipitation. When the amount of dissolved

mineral is larger than the quantity of existing mineral, then the mineral is considered to be exhausted. It is taken out of the chemical system for the next time step.

6.1 Relative increment in concentration

Sometimes concentrations of some species may vary tens of orders of magnitude. For instance, sulfate and sulfide concentrations change greatly from oxidizing to reducing conditions. This may lead to ill-conditioned Jacobian matrices and eventually to convergence failure. Basis switching, where most abundant species are dynamically switched as the set of components, can greatly improve the condition number of the Jacobian and help to overcome convergence problems (Wolery, 1992; Steefel and Lasaga, 1994). However, much more programming work and computing time is required if basis switching is tested everywhere and at every time step. The condition number of the matrix of a system of equations measures the sensitivity of the solution to modifications on the input data (Atkinson, 1989). The condition number times the relative error in the data provides an upper bound of the relative error in the solution. If the condition number is too large, the accuracy of the solution is poor and the significance of the results may be completely lost.

The Newton-Raphson iterative scheme implemented here uses relative concentration increments, $\Delta\mathbf{c}/\mathbf{c}$, or increments of log-concentrations, as unknowns rather than absolute increments, $\Delta\mathbf{c}$. The formulation is given in Appendix B. By working with relative increments and neglecting the derivatives of activity coefficients (see the following section), the Jacobian matrix is symmetric and invertible provided that primary species are the dominant species (as shown in Appendix B). In addition, it has a smaller condition number, especially for problems involving redox reactions in which some species such as dissolved oxygen may attain extremely low concentrations.

In the gypsum dissolution synthetic case, the condition number of the Jacobian matrix is equal to 1.35×10^{6} for absolute increments while it reduces to 3.2×10^{3} for relative increments. In the pyrite oxidation case the reduction in the condition number is even more dramatic (from 2.41×10^{10} to 7.63×10^{5}).

6.2 Neglecting derivatives of activity coefficients

The full Jacobian matrix includes terms involving derivatives of activity coefficients γ_j with respect to concentrations of primary species c_j. Activity coefficients depend on concentration of all primary species through ionic strength, which in turn involves concentrations of primary and secondary species, x_i. To evaluate $\frac{\partial \gamma_j}{\partial c_j}$ one has to compute $\frac{\partial \gamma_j}{\partial x_i}$ for all *i* which according to Eq. A4 in turn requires computing $\frac{\partial \gamma_j}{\partial c_j}$. A lengthy time-consuming iterative procedure is required for computing $\frac{\partial \gamma_j}{\partial c_j}$. In addition, the condition number of the Jacobian matrix sometimes may increase largely when derivatives of activity coefficients are considered. In the synthetic case involving pyrite oxidation, the condition number of **J** reduces from 4.31×10^{16} to 7.63×10^{5} when derivatives of activity coefficients are neglected. Such a reduction greatly enhances the convergence of the iterative procedure. Table 6 shows a comparison of the number of iterations and CPU time required to solve the gypsum dissolution synthetic problem for the following combinations: considering or not derivatives of activity coefficients and working with absolute and relative increments. The sequential iteration approach (SIA) was used always. The number of transport iterations is the same. No significant improvements are achieved in the number of chemical iterations and CPU time here by working with relative increments. As expected, the maximum number of chemical iterations is reduced when derivatives of activity coefficients are

considered. However, the total CPU time is increased. A 23% reduction of CPU time is achieved when derivatives of activity coefficients are neglected.

7. Conclusions

A sequential partly-iterative approach (SPIA) has been presented which only requires iteration between transport and chemical equations in areas where there is a large mass transfer between solid and liquid phases. Usually these areas coincide with system boundaries, moving reaction fronts and interfaces between different geochemical zones. This new approach (SPIA) as well as the sequential iterative, SIA, and non-iterative, SNIA, approaches were implemented in CORE^{2D}V4 a general 2-D finite element reactive transport code. The accuracy and numerical efficiency of SIA, SPIA and SNIA have been systematically analyzed using several synthetic cases and a case study involving reactive transport through the Llobregat Delta aquitard. The following conclusions can be drawn:

1) SNIA is numerically more efficient than SIA. SIA requires from 2 to 3 times as much CPU time as SNIA. The numerical solutions obtained with SNIA, however, are less accurate than SIA solutions and contain more numerical dispersion. SNIA errors depend on the type of chemical reactions and the grid Peclet and Courant numbers.

2) The new sequential partly-iterative approach, SPIA, requires less CPU time than SIA while its accuracy is comparable to that of SIA. On the other hand, SPIA is much more accurate than SNIA and requires only a slightly greater amount of CPU time. Accuracy of SPIA solutions depends on the partly-iterative tolerance ε. For $\varepsilon \leq 10^{-3}$, SPIA results are identical to those of SIA.

Several modifications of the standard Newton-Raphson iterative scheme used for solving the chemical equations have been proposed. These modifications include working with increments of log-concentrations and ignoring the terms of the Jacobian containing derivatives of activity

coefficients with respect to the concentrations of primary species. A proof has been given for the symmetry and nonsingularity of the Jacobian when such modifications are considered. It has been also shown numerically that both of them improve the efficiency and convergence of the iterative process and lead to better conditioned systems of equations.

As indicated by one of the reviewers, the accuracy and numerical efficiency of SIA, SPIA and SNIA should be analyzed in the future with the benchmark reactive transport problems listed in the MoMas group at http://www.gdrmomas.org/Ex_qualif/Geochimie/Documents/Benchmark-MoMAS.pdf.

Acknowledgments. CORE development and its applications have been funded by ENRESA, European Commission through FUNMIG (FP6-516514), NF-PPRO (FI6W-CT-2003-02389), FEBEX (FI4W-CT95-0006 & FIKW-CT-2000-0016), BENIPA (FIKW-CT-2000-00015), and CERBERUS (F14W-CT95-0008) projects of the Nuclear Fission Safety Programme, CICYT (HID98-0282 & REN2003-8882), Galician Research Program (PGIDT04PXIC11801PM & PGIDT00PX 111802) and University of La Coruña through a research scholarship awarded to the third author. Contributions of all professors and students to the development of CORE during the last 15 years as well as inputs of CORE users are greatly acknowledged. The second author was supported by the U.S. Dept. of Energy under Contract No. DE-AC02-05CH11231. We thank also the two anonymous reviewers for their comments and recommendations which have improved the paper.

References

Appelo, C.A.J., and Postma, D., 1993. Geochemistry, groundwater and pollution. Balkema, Rotterdam.

Appelo, C.A.J., 1994. Cation and proton exchange, pH variations and carbonate reactions in a freshening aquifer. Water Resour. Res., 30(10), 2793-2805.

Atkinson, K., 1989. An introduction to numerical analysis. John Wiley and Sons, New Jersey, 573 pp.

Ayora. C., Taberner, C., Saaltink, M.W., Carrera, J., 1998. The genesis of dedolomites: a discussion based on reactive transport modeling, J. Hydrol., 209, 346-365.

Cederberg, G.A., Street, R., Leckie, J.O., 1985. A groundwater mass transport and equilibrium chemistry model for multicomponent systems. Water Resour. Res., 21(8), 1095-1104.

Chilakapati, A., Yabusaki, S., Szecsody, J., MacEvoy, W., 2000. Groundwater flow, multicomponent transport and biogeochemistry: development and application of a coupled process model. Journal of Contaminant Hydrology, 43(3-4), 303-325.

Dai, Z., and Samper, J., 2004 Inverse problem of multicomponent reactive chemical transport in porous media: Formulation and applications: *Water Resour. Res.*, v. 40, p. W07407, doi: 10.1029/2004WR003248.

Dai Z. and J. Samper, 2006, Inverse modeling of water flow and multicomponent reactive transport in coastal aquifer systems: *J. of Hydrology*, doi:10.1016/j.jhydrol.2005.11.052, 327, 447-461.

Dai Z., J. Samper and R. Ritzi, 2006, Identifying geochemical processes by inverse modeling of multicomponent reactive transport in Aquia aquifer, Geosphere, Vol. 4, Nº 4, 210–219.

Engesgaard, P., 2000. Model for biological clogging in 3D, Brief user's manual and guide, Department of Hydrodynamics and Water Resources, Danish Technology University.

Galíndez, J.,M., J. Molinero, J. Samper and C.B Yang, 2006, Simulating concrete degradation processes by reactive transport models, J. Phys. IV France, Vol. 136, 177-188

Garboczi, E.J.,Bentz, D.P., 1992. Computer simulation of the diffusivity of cement-based materials. J. Mater. Sci., 27, 2083-2092

Ginn, T.R., Murphy, E.M., Chilakapati, A.,Seeboonruang, U., 2001. Stochastic-convective transport with nonlinear reaction and mixing: application to intermediate-scale experiments in aerobic biodegradation in saturated porous media. Journal of Contaminant Hydrology, 48(1-2), 121-149.

Herzer, J., Kinzelbach, W., 1989. Coupling of transport and chemical processes in numerical transport models. Geoderma, 44, 115-127.

Horn, R., Johnson, Ch., 1985. Matrix Analysis, Cambridge University Press, Cambridge.

Kaluarachchi, J.J.,Parker, J.C., 1990. Modeling multicomponent organic chemical transport in three-fluid-phase porous media. Journal of Contaminant Hydrology, 5(4), 349-374.

Kirkner, D.J., Jennings, A.A.,Theis, T.L., 1985. Multisolute mass transport with chemical interaction kinetics. Journal of Hydrology, 76(1-2), 107-117.

Lensing, H.J., Vogt, M.,Herrling, B., 1994. Modeling of biologically mediated redox processes in the subsurface. Journal of Hydrology, 159(1-4), 125-143.

Liu, C.W., Narasimhan, T.N., 1989. Redox-controlled multiple species reactive chemical transport, 2. Verification and Application. Water Resources Research, 25, 883-910.

Maher, K., Steefel, C.I., DePaolo, D.J.,Viani, B.E., 2006. The mineral dissolution rate conundrum: Insights from reactive transport modeling of U isotopes and pore fluid chemistry in marine sediments. Geochimica et Cosmochimica Acta, 70(2), 337-363.

Molinero, J., Samper, J., 2006. Modeling of reactive solute transport in fracture zones of granitic bedrocks, J Cont Hydrol 82, 293–318.

Molinero, J., Samper, J., Zhang, G., Yang, C., 2004. Biogeochemical reactive transport model of the redox zone experiment of the Äspö hard rock laboratory in Sweden. Nucl Technol 148, 151–165.

Nienhuis, P., Appelo, C.A.T.,Willemsen, A., 1991. Program PHREEQM: Modified from PHREEQM for use in mixing cell flow tube.

Pruess, K., Garcia, J., Kovscek, T., Oldenburg, C., Rutqvist, J., Steefel, C.,Xu, T., 2004. Code intercomparison builds confidence in numerical simulation models for geologic disposal of CO_2. Energy, 29(9-10), 1431-1444.

Regnier, P., O'Kane, J.P., Steefel, C.I.,Vanderborght, J.P., 2002. Modeling complex multi-component reactive-transport systems: towards a simulation environment based on the concept of a Knowledge Base. Applied Mathematical Modelling, 26(9), 913-927.

Richardson, I.G., 1999. The nature of C-S-H in hardened cements. Cement and Concrete Research 29, 1131–1147.

Saaltink, M.W., Ayora, C., Stuyfzand, P.J.,Timmer, H., 2003. Analysis of a deep well recharge experiment by calibrating a reactive transport model with field data. Journal of Contaminant Hydrology, 65(1-2), 1-18.

Saaltink, M.W., Carrera, J., Ayora, C., 2000. A comparison of two approaches for reactive transport modelling. Journal of Geochemical Exploration, 69-70, 97-101.

Salvage, K.M.,Yeh, G.-T., 1998. Development and application of a numerical model of kinetic and equilibrium microbiological and geochemical reactions (BIOKEMOD). Journal of Hydrology, 209(1-4), 27-52.

Samper J., Juncosa R., Delgado J. and Montenegro L. (2000) CORE^{2D}: A code for non-isothermal water flow and reactive solute transport. Users manual version 2. ENRESA Technical Publication 06/2000: 131 pp.

Samper, J., Yang, C., Montenegro, L., 2003. CORE^{2D} version 4: A code for non-isothermal water flow and reactive solute transport. Users Manual. University of La Coruña, Spain.

Samper J., Yang, C., 2006. Stochastic analysis of transport and multicomponent competitive monovalent cation exchange in aquifers. Geosphere 2, 102-112.

Samper, J., Zhang, G., Montenegro, L., 2006a. Coupled microbial and geochemical reactive transport models in porous media: Formulation and application to synthetic and *in situ* experiments. J Iberian Geology 32 (2), 215-231.

Samper, J., C. Yang, A. Naves, A Yllera, A. Hernández, J. Molinero, J. M. Soler, P. Hernán, J.C. Mayor and J. Astudillo, 2006b, A fully 3-D anisotropic model of DI-B *in situ* diffusion experiment in the Opalinus clay formation, Physics and Chemistry of the Earth, Vol. 31, 531-540.

Samper, J.,Yang, C., 2007. An approximate analytical solution for multicomponent cation exchange reactive transport in Groundwater. Transport in Porous Media, 69, 67-88.

Samper, J., L. Zheng, A.M. Fernández and L. Montenegro, 2008a, Inverse modeling of multicomponent reactive transport through single and dual porosity media, J Cont Hydrol, Vol 98/3-4 pp 115-127.

Samper, J., L. Zheng, and L. Montenegro 2008b, Inverse hydrochemical models of aqueous extract experiments, Physics and Chemistry of the Earth, doi:10.1016/j.pce.2008.05.012.

Samper J., L. Zheng, L. Montenegro, A.M. Fernández, & P. Rivas, 2008c, Testing coupled thermo-hydro-chemical models of compacted bentonite after dismantling the FEBEX in situ test, Appl Geochem, Vol 23/5: 1186-1201. doi:10.1016/j.apgeochem.2007.11.010.

Steefel, C.I., 1993. 1DREACT, One dimensional reaction-transport model, User manual and programmer's guide, Pacific Northwest Laboratories, Batelle, Washington.

Steefel, C.I., DePaolo, D.J.,Lichtner, P.C., 2005. Reactive transport modeling: An essential tool and a new research approach for the Earth sciences. Earth and Planetary Science Letters, 240(3-4), 539-558.

Steefel, C.I.,Lichtner, P.C., 1994. Diffusion and reaction in rock matrix bordering a hyperalkaline fluid-filled fracture. Geochimica et Cosmochimica Acta, 58(17), 3595-3612.

Steefel, C.I., Lasaga, A.C., 1994. A coupled model for transport of multiple chemical species and kinetic precipitation/dissolution reactions with applications to reactive flow in single phase hydrothermal system. Am. J. Sci., 294, 529-592.

Steefel, C.I. MacQuarrie, K.T.B., 1996. Approaches to modelling of reactive transport in porous media, In: Reactive transport in porous media. Reviews in Mineralogy, vol. 34, 83-129, Mineralogical Society of America.

Steefel, C.I.,Lichtner, P.C., 1998. Multicomponent reactive transport in discrete fractures: II: Infiltration of hyperalkaline groundwater at Maqarin, Jordan, a natural analogue site. Journal of Hydrology, 209(1-4), 200-224.

Steefel, C.I.,Van Cappellen, P., 1990. A new kinetic approach to modeling water-rock interaction: The role of nucleation, precursors, and Ostwald ripening. Geochimica et Cosmochimica Acta, 54(10), 2657-2677.

Stumm, W., Morgan, J.J., 1981. Aquatic chemistry: an introduction emphasizing chemical equilibria in natural waters. John Wiley and Sons, New York.

Tebes-Stevens, C., J. Valocchi, A., VanBriesen, J.M.,Rittmann, B.E., 1998. Multicomponent transport with coupled geochemical and microbiological reactions: model description and example simulations. Journal of Hydrology, 209(1-4), 8-26.

Valocchi, A.J., Malmstead, M., 1992. A note on the accuracy of operator splitting for advection-dispersion-reaction problems. Water Resour. Res., 28(5), 1471-1476.

Xu, T., 1996. Modeling non-isothermal multicomponent reactive solute transport through variably saturated porous media. Ph.D. Dissertation, University of La Coruña, La Coruña, Spain.

Xu, T., J. Samper, C. Ayora, M. Manzano and E. Custodio, 1999 Modeling of non-isothermal multicomponent reactive transport in field scale porous media flow systems, *J Hydrol*, Vol. 214, 144-164.

Xu T., S.P. White, K. Pruess and G.H. Brimhall G.H., 2000, Modeling of pyrite oxidation in saturated and unsaturated subsurface flow systems. Transport in Porous Media. 39(1):25-56.

Walter, A.L., Frind, E.O., Blowes, D.W., Ptacek, C.J., Molson, J.W., 1994. Modeling of multicomponent reactive transport in groundwater, 1, Model development and evaluation. Water Resour. Res., 30 (11), 3137-3148.

Wolery, T.J., 1992. EQ3NR, a computer program for geochemical aqueous speciation-solubility calculations (version 7.0), Lawrence Livermore Laboratory

Yabusaki, S.B., Steefel, C.I.,Wood, B.D., 1998. Multidimensional, multicomponent, subsurface reactive transport in nonuniform velocity fields: code verification using an advective reactive streamtube approach. Journal of Contaminant Hydrology, 30(3-4), 299-331.

Yang, C., 2006. Conceptual and numerical coupled thermal-hydro-bio-geochemical models for three-dimensional porous and fractured media. Ph.D. Thesis, Univ. of La Coruña, La Coruña, Spain.

Yang, C., Samper, J., Molinero, J., Bonilla, M., 2007. Modelling geochemical and microbial consumption of dissolved oxygen after backfilling a high level radiactive waste repository. Journal of Contaminant Hydrology, 93, 130-148.

Yang, C., Samper, J.,Montenegro, L., 2008a. A coupled non-isothermal reactive transport model for long-term geochemical evolution of a HLW repository in clay. Environmental Geology 53, 1627-1638.

Yang, C., Samper, J., Molinero, J, 2008b. Inverse microbial and geochemical reactive transport models in porous media, Physics and Chemistry of the Earth, accepted, in press.

Yang, C.,Samper, J., 2008. A subgrid scale stabilized finite element method to multicomponent reactive transport in porous media. Transport in Porous Media, accepted, in press.

Yeh, G.T., Tripathi, V.S., 1989. A critical evaluation of recent developments of hydrogeochemical transport models of reactive multichemical components. Water Resour. Res. 25(1), 93-108.

Yeh, G. T. and V. S. Tripathi, 1991. A model for simulating transport of reactive multispecies components: Model development and demonstration. Water Resour. Res. Vol. 27, No. 12, 3075-3094.

Yeh, G.T., 2000. Computational subsurface hydrology, reactions, transport and fate of chemicals and microbes. Kluwer Acdemic Publishers, The Netherland.

Zhang, G., 2001. Nonisothermal hydrobiogeochemical models in porous media. Ph.D. Diss. Thesis, University of A Coruña, La Coruña, Spain.

Zhang, G., Samper, J., Montenegro L., 2008. Coupled thermo-hydro-bio-geochemical reactive transport model of the CERBERUS heating and radiation experiment in Boom clay. Applied Geochemistry 23, 932-949.

Appendix A: Solution of the chemical equations

The proposed numerical formulation for solving the chemical equations can be applied to problems involving homogeneous (aqueous complexation, acid-base and redox) and heterogeneous reactions (mineral dissolution/precipitation, gas dissolution/ex-solution, cation exchange and adsorption). For the sake of simplicity, the formulation presented here is restricted to systems involving only aqueous complexation and mineral dissolution/precipitation reactions. The general formulation can be found in Xu (1996). The formulation is based on mass balances in terms of components (Yeh and Tripathi, 1991). The total analytical concentration of the j-th component, T_j, in the system is given by

$$T_j = c_j + \sum_{i=1}^{N_x} \nu_{ij}^x x_i + \sum_{m=1}^{N_p} \nu_{mj}^p p_m \qquad j = 1, ..., N_C \qquad \text{(A1)}$$

which includes the concentration of the j–th component, c_j, as well as the contributions, x_i, of the N_x aqueous complexes and p_m corresponding to the N_p mineral phases. ν_{ij}^x and ν_{mj}^p are the stoichiometric coefficients of the j-th component in the i-th aqueous complex and m-th mineral, respectively. The sum of the first two terms of the right-hand side of (A1) are total dissolved component concentrations, C_j

$$C_j = c_j + \sum_{i=1}^{N_X} \nu_{ij}^x x_i \qquad j = 1, \ldots, N_C \qquad \text{(A2)}$$

which are subject to transport (see Eq. 1). By lumping all the terms in the right-hand side of (A1) into a single term F_j^c, one has:

$$F_j^c = c_j + \sum_{i=1}^{N_x} \nu_{ij}^x x_i + \sum_{m=1}^{N_p} \nu_{mj}^p p_m - T_j = 0 \qquad j = 1, ..., N_C \qquad \text{(A3)}$$

The local equilibrium assumption provides an explicit expression for the concentrations of aqueous complexes, x_i, in terms of component concentrations, c_j:

$$x_i = K_i^{-1}\gamma_i^{-1}\prod_{j=1}^{N_C} c_j^{\nu_{ij}^x}\gamma_j^{\nu_{ij}^x} \qquad \text{(A4)}$$

where γ_j and γ_i are thermodynamic activity coefficients, and K_i is the equilibrium constant. There is no such an explicit expression relating the concentration of precipitated species, p_m, to c_j (Yeh and Tripathi, 1991). Instead, one has a mass-action equation for the m-th mineral which can be written as:

$$F_m^p = K_m^{-1}\prod_{j=1}^{N_C} c_j^{\nu_{mj}^p}\gamma_j^{\nu_{mj}^p} - 1 = 0 \qquad m = 1,\ldots,N_P \qquad \text{(A5)}$$

where K_m is the m-th mineral solubility (equilibrium) constant. These N_P equations plus the N_C equations in (A3) provide the set of equations required to solve for the (N_C+N_P) unknowns $(c_1, c_2, \ldots, c_{N_C}, p_1, p_2, \ldots, p_{N_p})$ which are lumped into a column vector **X** having entries, X_l (l=1, 2,..., N_C+N_P). In the Newton-Raphson method, the unknowns are computed iteratively according to

$$X_l^{n+1} = X_l^n + \Delta X_l \qquad \text{(A6)}$$

where n denotes iteration number and ΔX_l are changes in unknowns which are obtained by solving the following system of linear equations

$$\sum_{i=1}^{N_C+N_P} \frac{\partial F_l}{\partial X_i}\Delta X_i = -F_l \qquad l = 1\ldots N_C + N_P \qquad \text{(A7)}$$

which in matrix form reduces to

$$\mathbf{J}\,\Delta\mathbf{X} = -\mathbf{F} \qquad \text{(A8)}$$

where **F** and Δ**X** are column vectors of residuals and unknowns, respectively, and **J** is the Jacobian matrix which contains the derivatives of the residuals F_l with respect to the unknowns, X_i. Its evaluation is described in Appendix B. The iterative process in (A6) is repeated until a prescribed convergence tolerance is satisfied.

Appendix B: The Jacobian matrix for solving chemical equations

The Jacobian matrix for aqueous complexation and mineral dissolution/precipitation reactions is given by:

$$\begin{array}{c} \\ N_C \\ N_P \end{array} \begin{array}{c} \begin{array}{cc} N_C & N_P \end{array} \\ \begin{pmatrix} \dfrac{\partial F_j^c}{\partial c_\lambda} & \dfrac{\partial F_j^c}{\partial p_\mu} \\ \dfrac{\partial F_m^p}{\partial c_\lambda} & \dfrac{\partial F_m^p}{\partial p_\mu} \end{pmatrix} \end{array}$$

By substituting (A4) into (A3) and taking derivatives of the resulting expression with respect to c_λ and p_μ, one has

$$\frac{\partial F_j^c}{\partial c_\lambda} = \left[\delta_{j\lambda} + \sum_{i=1}^{N_x} \nu_{ij}^x \nu_{i\lambda}^x \frac{x_i}{c_\lambda} \right] \tag{B1}$$

$$\frac{\partial F_j^c}{\partial p_\mu} = \nu_{\mu j}^p \tag{B2}$$

where derivatives of activity coefficients with respect to c_λ have been neglected. The remaining blocks of the Jacobian matrix are obtained by taking derivatives of (A5) with respect to c_λ and p_μ:

$$\frac{\partial F_m^p}{\partial c_\lambda} = \frac{\nu_{m\lambda}^p}{c_\lambda} \tag{B3}$$

$$\frac{\partial F_m^p}{\partial p_\mu} = 0 \tag{B4}$$

Let $\mathbf{J}^{cc}$, $\mathbf{J}^{cp}$, $\mathbf{J}^{pc}$ and $\mathbf{J}^{pp}$ be the blocks of $\mathbf{J}$ in Eqs. B1 through B4. The system of equations (A8) can be written as

$$\begin{bmatrix} \mathbf{J}^{cc} & \mathbf{J}^{cp} \\ \mathbf{J}^{pc} & \mathbf{J}^{pp} \end{bmatrix} \begin{bmatrix} \mathbf{\Delta c} \\ \mathbf{\Delta p} \end{bmatrix} = \begin{bmatrix} -\mathbf{F}^c \\ -\mathbf{F}^p \end{bmatrix} \tag{B5}$$

where $-\mathbf{F}^c$ and $-\mathbf{F}^p$ are the residual terms which can be calculated from Eqs. A3 and A5, respectively. It should be noticed that this formulation of the Newton-Raphson equations does not yield a symmetric Jacobian matrix because neither the diagonal block $\mathbf{J}^{cc}$ is symmetric nor $\mathbf{J}^{pc}$ is the transpose of $\mathbf{J}^{cp}$. However, by introducing the concept of relative concentration increments, $\Delta\mathbf{c}/\mathbf{c}$, which coincide with increments of log-concentrations, Eq. B5 can be rewriten as

$$\begin{bmatrix} (\mathbf{J}^{cc})^* & \mathbf{J}^{cp} \\ (\mathbf{J}^{pc})^* & \mathbf{J}^{pp} \end{bmatrix} \begin{bmatrix} \mathbf{\Delta c/c} \\ \mathbf{\Delta p} \end{bmatrix} = \begin{bmatrix} -\mathbf{F}^c \\ -\mathbf{F}^p \end{bmatrix} \tag{B6}$$

where

$$(\mathbf{J}^{cc})^*_{j\lambda} = \left[\delta_{j\lambda} c_\lambda + \sum_{i=1}^{N_x} \nu^x_{ij} \nu^x_{i\lambda} x_i \right] \tag{B7}$$

$$(\mathbf{J}^{pc})^*_{m\lambda} = \nu^p_{m\lambda} \tag{B8}$$

By working with relative increments, the Jacobian matrix becomes symmetric because both diagonal blocks $(\mathbf{J}^{cc})^*$ and $\mathbf{J}^{pp}$ are symmetric (in fact $\mathbf{J}^{pp}$ is the null matrix), and $(\mathbf{J}^{pc})^*$ coincides with the transpose of $\mathbf{J}^{cp}$. Notice also that if primary species are taken as the most abundant aqueous species, then $c_j >> x_i$ for all i. Under these conditions, the block $(\mathbf{J}^{cc})^*$ is diagonally dominant, a property that according to the Levy-Desplanques theorem (Horn and Johnson, 1985) provides a sufficient condition for $(\mathbf{J}^{cc})^*$ to be invertible. Furthermore, $\mathbf{J}^{cp}$ is a $N_C x N_P$ matrix having entries equal to the stoichiometric coefficients of the N_c primary species in the N_P mineral phases. According to the phase rule (Stumm and Morgan, 1981), $N_P \leq N_C$. Since mineral phases are linearly independent, the rank of matrix $\mathbf{J}^{cp}$ is equal to N_P. This ensures that the rank of matrix $\mathbf{B}$ ($N_P x N_P$) defined as

$$\mathbf{B} = \left(\mathbf{J}^{cp}\right)^t \left(\mathbf{J}^{cc*}\right)^{-1} \mathbf{J}^{cp} \tag{B9}$$

is also equal to N_P (Horn and Johnson, 1985). This is a sufficient condition for $\mathbf{B}$ to be invertible which allows one to compute the inverse of the Jacobian in (B6) according

$$\mathbf{J}^{-1} = \begin{pmatrix} \left(\mathbf{J}^{cc*}\right)^{-1} - \mathbf{A}\mathbf{B}^{-1}\mathbf{A}^{t} & \mathbf{A}\mathbf{B}^{-1} \\ \mathbf{B}^{-1}\mathbf{A}^{t} & -\mathbf{B}^{-1} \end{pmatrix} \tag{B10}$$

where

$$\mathbf{A} = \left(\mathbf{J}^{cc*}\right)^{-1}\mathbf{J}^{cp} \tag{B11}$$

Table 1. Summary of maximum and average relative differences of computed concentrations with sequential non-iterative (SNIA) and sequential partly-iterative (SPIA) with respect to the sequential iterative approach (SIA) for four synthetic cases. A convergence tolerance, ε in Eq. 10, of 10^{-3} was used for all SPIA runs.

Case	δ_{max}^{SPIA} (%) (see Eq. 12)	$\bar{\delta}^{SPIA}$ (%) (see Eq. 13)	δ_{max}^{SNIA} (%) (see Eq. 12)	$\bar{\delta}^{SNIA}$ (%) (see Eq. 13)
Dissolution	9×10^{-5}	3×10^{-5}	0.272	0.124
Redox	5.3×10^{-4}	9×10^{-5}	0.846	0.214
Adsorption	4.1×10^{-4}	1.3×10^{-4}	1.158	0.392
Exchange	8.4×10^{-4}	9×10^{-5}	57.4	2.4

Table 2. Comparison of CPU times (minutes in a Pentium PC 266 computer) required by SIA, SPIA and SNIA for several synthetic cases.

Case	SIA	SPIA	SNIA	Ratio SIA/SNIA	Ratio SPIA/SNIA
Dissolution	1.18	0.67	0.45	2.62	1.48
Redox	0.21	0.18	0.15	1.40	1.20
Adsorption	2.63	1.72	1.14	2.30	1.50
Exchange	16.4	8.24	4.315	3.80	1.90

Table 3. Total dissolved component concentrations (mmol/l) of initial and bottom boundary water solutions (adapted from Manzano, 1993). X denotes exchange sites (in meq/l).

	Cl	C	S	Na	K	Ca	Mg	N	pH	X
Initial	613.2	32.0	8.5	521.9	12.8	5.0	32.6	15.0	7.9	645.3
Boundary	5.01	32.0	0.4	51.7	2.74	1.8	3.0	0.9	6.8	_

Table 4. List of hydrogeochemical reactions considered in the reactive transport model of the Llobregat Delta aquitard. Here "-X" denotes a cation exchange site.

Geochemical reactions	$\log_{10}$(K) at 25 ^{o}C
Aqueous dissociation:	
$OH^- = H_2O - H^+$	13.995
$CO_3^{2-} = HCO_3^- - H^+$	10.329
$CO_2(aq) = HCO_3^- + H^+ - H_2O$	-6.3447
$CaHCO_3^+ = Ca^{2+} + HCO_3^-$	-1.0467
$MgHCO_3^+ = Mg^{2+} + HCO_3^-$	-1.0357
$CaCO_3(aq) = Ca^{2+} + HCO_3^- - H^+$	7.0017
$MgCO_3(aq) = Mg^{2+} + HCO_3^- - H^+$	7.3499
$NaHCO_3(aq) = Na^+ + HCO_3^-$	-0.1541
$CaSO_4(aq) = Ca^{2+} + SO_4^{2-}$	-2.1111
$MgSO_4(aq) = Mg^{2+} + SO_4^{2-}$	-2.309
$NaSO_4^- = Na^+ + SO_4^{2-}$	-0.82
$KSO_4^- = K^+ + SO_4^{2-}$	-0.8796
Cation exchange:	
$Na^+ + 0.5Ca\text{-}X_2 = 0.5Ca^{2+} + Na\text{-}X$	0.1543
$Na^+ + 0.5Mg\text{-}X_2 = 0.5Mg^{2+} + Na\text{-}X$	0.2697
$Na^+ + K\text{-}X = K^+ + Na\text{-}X$	0.3626
$Na^+ + NH_4\text{-}X = NH_4^+ + Na\text{-}X$	0.5
mineral dissolution-precipitation:	
$CaCO_3(s)$ (Calcite) $= Ca^{2+} + HCO_3^- - H^+$	1.8487

Table 5. CPU time required by SNIA, SPIA and SIA to solve reactive transport through the Llobregat Delta aquitard for different Peclet and Courant numbers.

Peclet number	Courant number	CPU time			SPIA/SNIA	SIA/SNIA	SPIA/SIA
		SNIA	SPIA	SIA			
0.5	0.0579	4.79	5.12	9.13	1.06	1.90	0.56
0.5	0.2316	1.45	2.82	4.31	1.94	2.97	0.65
0.5	0.4632	0.85	1.85	2.51	2.17	2.95	0.73
0.5	0.9264	0.61	1.36	1.92	2.22	3.14	0.71
1.0	0.0579	5.17	5.28	9.71	1.02	1.87	0.54
1.0	0.2316	1.43	2.65	3.89	1.85	2.72	0.68
1.0	0.4632	0.92	1.94	2.63	2.10	2.85	0.74
1.0	0.9264	0.52	1.35	1.64	2.59	3.15	0.82
2.0	0.0579	5.21	5.58	10.56	1.07	2.02	0.53
2.0	0.2316	1.47	1.53	2.47	1.04	1.68	0.62
2.0	0.4632	0.93	1.87	2.62	2.01	2.82	0.71
2.0	0.9264	0.59	1.59	2.17	2.69	3.68	0.73

Table 6. Comparison of number of iterations and CPU time required when derivatives of activity coefficients are considered (CDAC) or not (NO CDAC) and by working with relative (RIC) and absolute increments (AIC) for the gypsum dissolution synthetic case.

	Number of transport iterations	Number of chemistry iterations	CPU time
AIC + CDAC	1-3	3-4	1.39
AIC + NO CDAC	1-3	3-6	1.18
RIC + CDAC	1-3	3-4	1.37
RIC + NO CDAC	1-3	3-7	1.13

Figure captions

Figure 1. Log-log plot of maximum and average relative differences, δ^*_{max} and $\overline{\delta}^*$ (in Eq. 12 and 13), in concentrations computed with SNIA, SPIA (with a convergence tolerance ε of 10^{-2}), and SIA as a function of Courant number for the cation exchange case using Peclet numbers of 0.2 and 1.

Figure 2. Concentration breakthrough curves computed with SIA, SPIA and SNIA for the cation exchange case using Courant and Peclet numbers equal to 1.

Figure 3. Log-log plot of maximum and average relative differences, δ^*_{max} and $\overline{\delta}^*$ (in Eq. 12 and 13), in the concentrations computed with SNIA and SIA as a function of Courant number for the Llobregat Delta aquitard. Results are shown for Peclet numbers, P, of 0.5, 1 and 2.

Figure 4. Concentration breakthrough curves computed with SIA, SPIA and SNIA approaches at several depths of the Llobregat Delta aquitard using Courant and Peclet numbers equal to one. Aquitard bottom is at a depth of 36 m. Notice that the concentration scale in Figure 4d is ten times larger than those of Figures 4a, 4b and 4c.

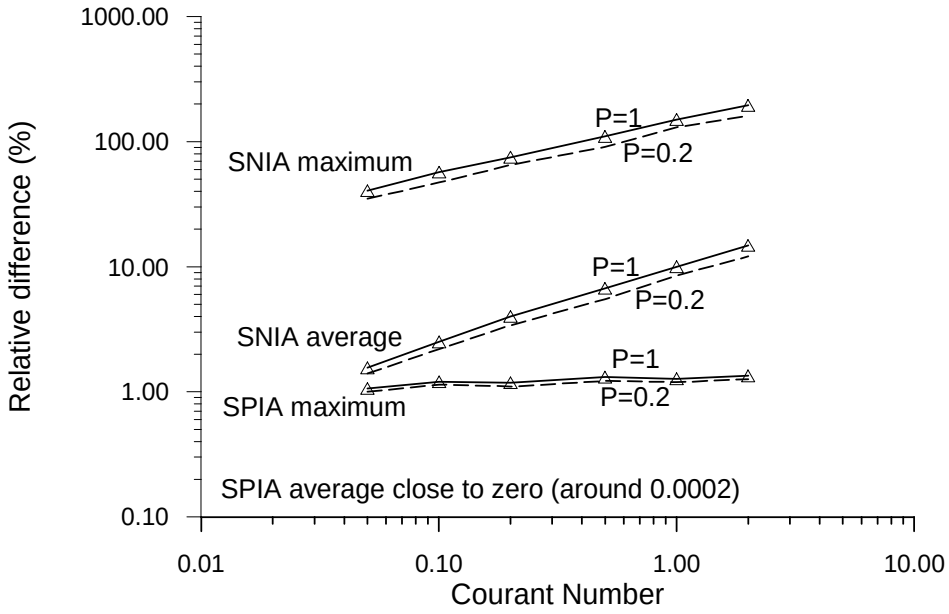

Figure 1.

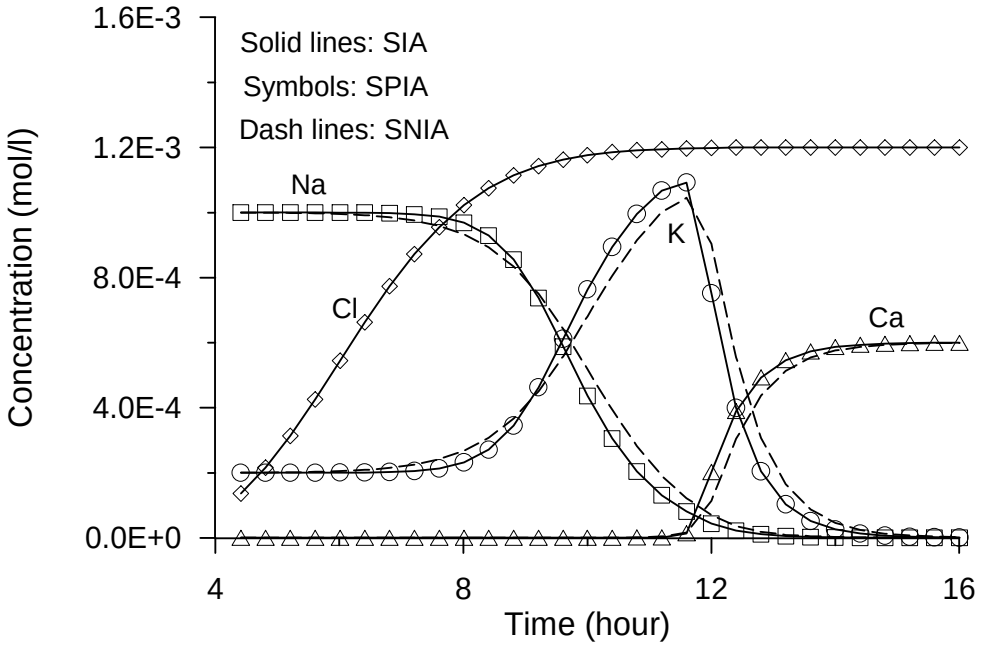

Figure 2.

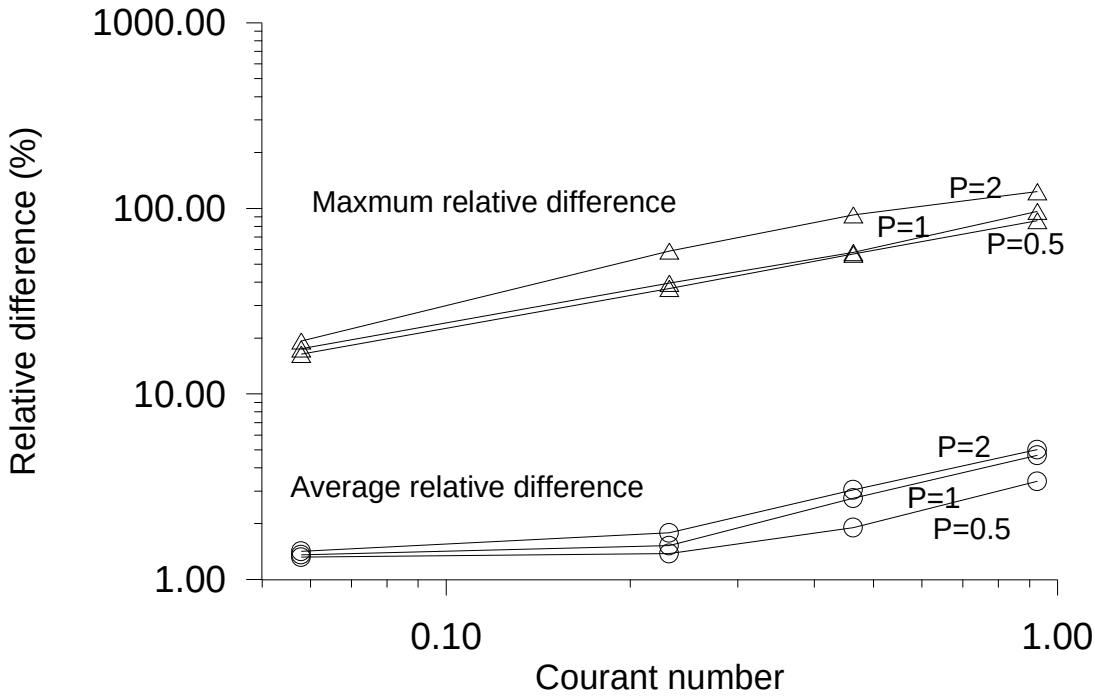
1000.00
100.00
10.00
1.00
Relative difference (%)
Maxmum relative difference
P=2
P=1
P=0.5
Average relative difference
P=2
P=1
P=0.5
0.10
1.00
Courant number

Figure 3.

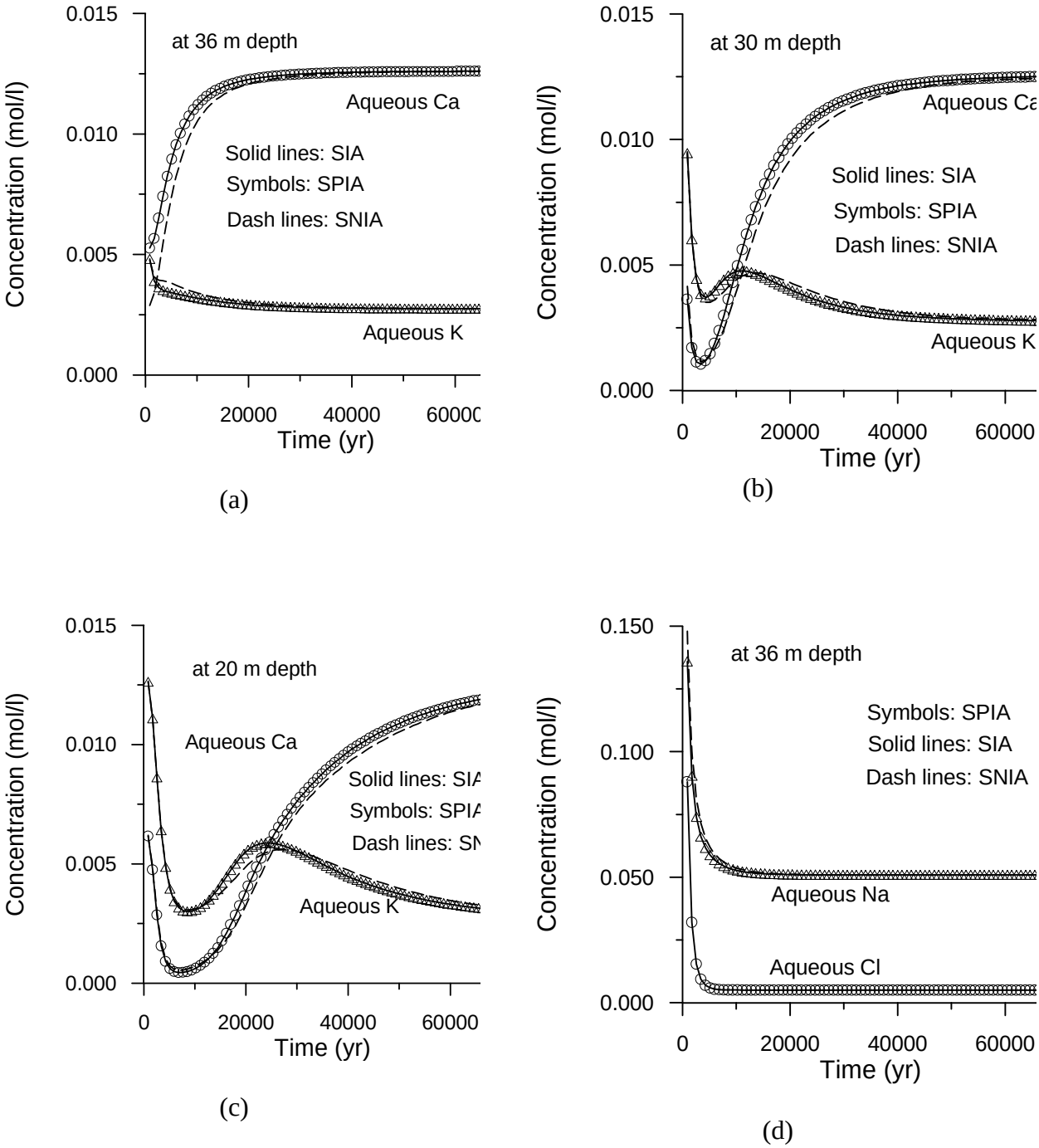
0.015
0.010
0.005
0.000
Concentration (mol/l)
at 36 m depth
Aqueous Ca
Solid lines: SIA
Symbols: SPIA
Dash lines: SNIA
Aqueous K
0
20000
40000
60000
Time (yr)
(a)
at 30 m depth
Aqueous Ca
Solid lines: SIA
Symbols: SPIA
Dash lines: SNIA
Aqueous K
Time (yr)
(b)
at 20 m depth
Aqueous Ca
Solid lines: SIA
Symbols: SPIA
Dash lines: SNIA
Aqueous K
Time (yr)
(c)
0.150
0.100
0.050
at 36 m depth
Symbols: SPIA
Solid lines: SIA
Dash lines: SNIA
Aqueous Na
Aqueous Cl
Time (yr)
(d)

Figure 4.